

## Geological and geomorphological analysis of a complex landslides system: the case of San Martino sulla Marruccina (Abruzzo, Central Italy)

Francesca Bozzano, Cristiano Carabella, Pierfederico De Pari, Marco Emanuele Discenza, Rosanna Fantucci, Paolo Mazzanti, Enrico Miccadei, Alfredo Rocca, Sergio Romano & Nicola Sciarra

To cite this article: Francesca Bozzano, Cristiano Carabella, Pierfederico De Pari, Marco Emanuele Discenza, Rosanna Fantucci, Paolo Mazzanti, Enrico Miccadei, Alfredo Rocca, Sergio Romano & Nicola Sciarra (2019): Geological and geomorphological analysis of a complex landslides system: the case of San Martino sulla Marruccina (Abruzzo, Central Italy), Journal of Maps, DOI: [10.1080/17445647.2019.1702596](https://doi.org/10.1080/17445647.2019.1702596)

To link to this article: <https://doi.org/10.1080/17445647.2019.1702596>



© 2019 The Author(s). Published by Informa UK Limited, trading as Taylor & Francis Group on behalf of Journal of Maps



[View supplementary material](#)



Published online: 18 Dec 2019.



[Submit your article to this journal](#)



[View related articles](#)



[View Crossmark data](#)



## Geological and geomorphological analysis of a complex landslides system: the case of San Martino sulla Marrucina (Abruzzo, Central Italy)

Francesca Bozzano <sup>a,b</sup>, Cristiano Carabella <sup>c</sup>, Pierfederico De Pari<sup>d</sup>, Marco Emanuele Discenza <sup>d</sup>, Rosanna Fantucci<sup>e</sup>, Paolo Mazzanti <sup>a,b</sup>, Enrico Miccadei <sup>c</sup>, Alfredo Rocca <sup>b</sup>, Sergio Romano<sup>d</sup> and Nicola Sciarra <sup>c</sup>

<sup>a</sup>Department of Earth Science, School of Mathematical, Physical and Natural Sciences, "Sapienza" University of Rome, Roma, Italy; <sup>b</sup>NHAZCA s.r.l. Spin-Off of Sapienza University of Rome, Roma, Italy; <sup>c</sup>Department of Engineering and Geology, Università degli Studi "G. d'Annunzio" Chieti-Pescara, Laboratory of Tectonic Geomorphology and GIS, Chieti Scalo, Italy; <sup>d</sup>Geoservizi s.r.l. Ripalimosani, Italy; <sup>e</sup>Geologi Associati Fantucci e Stocchi, Viterbo, Italy

### ABSTRACT

This work deals with the landslides affecting the area surrounding the village of San Martino sulla Marrucina and involving the neighboring municipalities of Casacanditella and Filetto. The geological and geomorphological settings of this area are being discussed. The enclosed maps have been realized following a multidisciplinary approach, based on morphometric, geological, and geomorphological analyses and supported by air-photo interpretation, dendrochronology, and satellite SAR interferometry (InSAR). The map is organized in four sections: orography (on the upper part), geological map (on the upper right part), main geomorphological map (in the central left part, 1:7,500 scale), and multitemporal analysis (in the lower part). The aforementioned multi-temporal assessment of landslides was performed according to the geomorphological evidence-based criteria and the past ground displacement measurements were obtained by dendrochronology and InSAR. The aim of the study is to understand the evolution in time and space of this landslide area, focusing on the corresponding kinematics.

### ARTICLE HISTORY

Received 16 September 2019  
Revised 15 November 2019  
Accepted 5 December 2019

### KEYWORDS

Landslides;  
geomorphological mapping;  
air-photo interpretation;  
dendrochronology; satellite  
SAR interferometry (InSAR);  
Central Apennines


## 1. Introduction

Landslides play an important role in the landscape evolution and represent a serious hazard in many areas of the World (Aleotti & Chowdhury, 1999; Dai, Lee, & Ngai, 2002; Glade, Anderson, & Crozier, 2012). These phenomena are widespread in large areas of the Italian territory (Brunetti et al., 2010; Peruccacci et al., 2017; Salvati, Bianchi, Rossi, & Guzzetti, 2010) and mainly in the Abruzzo piedmont area (Central Italy). Many areas are very prone to landslide, due to the combination of their peculiar morphological, geological, climatic characteristics, and to the destabilizing effects induced by human activity (Carabella, Miccadei, Paglia, & Sciarra, 2019; Calista, Miccadei, Piacentini, & Sciarra, 2019; Francioni et al., 2019; Peruccacci, Brunetti, Luciani, Vennari, & Guzzetti, 2012).

Geomorphological mapping is a common and fundamental tool for the representation of landforms and their evolution, with special reference to landslides. It is particularly significant for the comprehension of the time development of landslides and becomes the source document to perform different typologies of analysis, especially in the case of large complex landslides

systems. Multitemporal investigations allow for the analysis of multiple activation, mechanisms, and evolution of landslides. Depending on the final purpose, several types of landslide mapping can be achieved and realized through various techniques: landslide inventory, landslide typology, and landslide state of activity maps. Standard methods include field survey and visual interpretation of stereoscopic aerial photographs (see, e.g. Calista et al., 2019; Piacentini, Galli, Marsala, & Miccadei, 2018). Other valid methods and data employed for landslide mapping comprise the use of LIDAR (Laser Imaging Detection and Ranging) data (Gaidzik et al., 2017; Höfle & Rutzinger, 2011; Jaboyedoff et al., 2012), whereas those exploited for the state of activity analysis incorporate dendrochronological data (Coulthard & Smith, 2013; Pezzo & Dorigatti, 1999), and Synthetic Aperture Radar (SAR) data (Amato et al., 2017; Del Ventisette, Righini, Moretti, & Casagli, 2014; Ferretti, Prati, & Rocca, 2001; Perissin & Wang, 2012) as ancillary data in order to improve geomorphological analyses and to monitor landslides evolution (Akbarimehr, Motagh, & Haghshenas-Haghighi, 2013; Bardi et al., 2014; Bozzano et al., 2017; Ciolli et al.,

**CONTACT** Enrico Miccadei  enrico.miccadei@unich.it  Department of Engineering and Geology, Università degli Studi "G. d'Annunzio" Chieti-Pescara, Laboratory of Tectonic Geomorphology and GIS, Via dei Vestini 31, 66100 Chieti Scalo (CH), Italy

 Supplemental data for this article can be accessed <https://doi.org/10.1080/17445647.2019.1702596>

© 2019 The Author(s). Published by Informa UK Limited, trading as Taylor & Francis Group on behalf of Journal of Maps

This is an Open Access article distributed under the terms of the Creative Commons Attribution License (<http://creativecommons.org/licenses/by/4.0/>), which permits unrestricted use, distribution, and reproduction in any medium, provided the original work is properly cited.

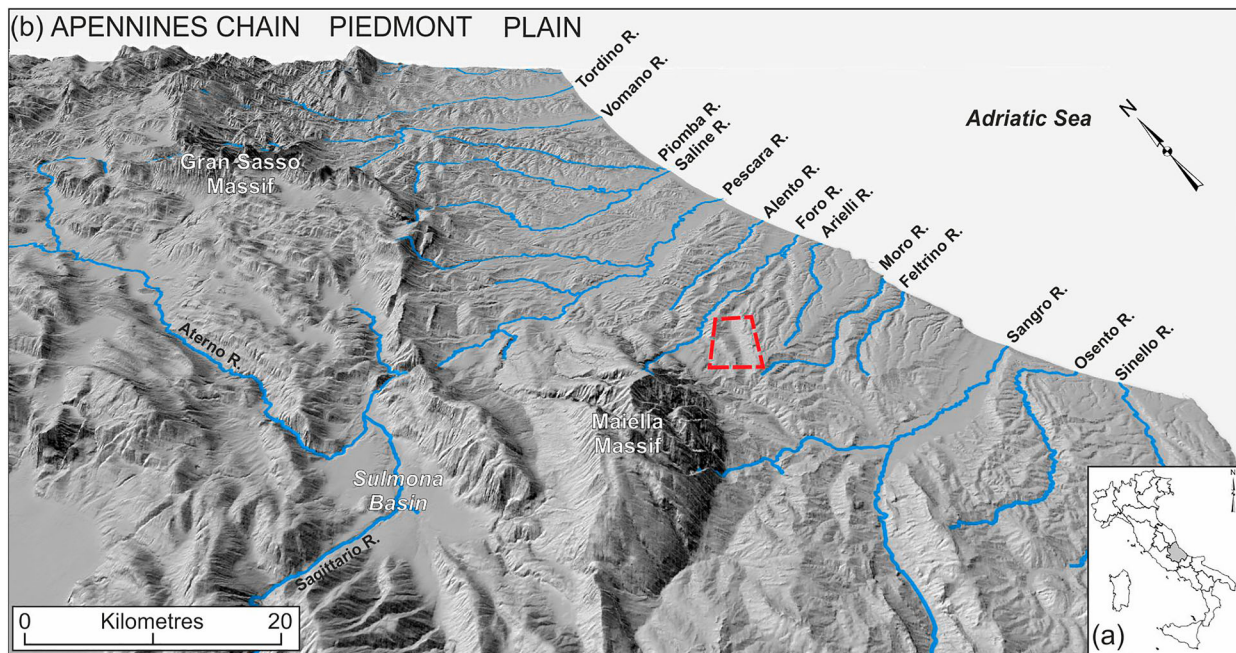


**Figure 1.** (a) Location map of the study area in Central Italy; (b) three-dimensional view (from 20 m DEM, SINAnet) of the Abruzzo Region. The red-dashed box indicates the location of the study area.

2019; Fantucci & Sorriso-Valvo, 1999; Stefanini, 2004; Tofani, Raspini, Catani, & Casagli, 2013).

This work focused on the multidisciplinary analysis of a large landslide area located in Central Italy, in the eastern Abruzzo Apennines piedmont, near the villages of San Martino sulla Marrucina, Casacanditella, and Filetto (Figure 1).

This study is the outcome of a detailed geological and geomorphological investigations, combined with aerial photos interpretation, borehole log-stratigraphy, dendrochronological data, and satellite interferometric analysis. This integrated survey allowed for a comprehensive description of the geomorphological features of the large landslides area near San Martino sulla Marrucina, as well as for the definition of the recent geomorphological evolution.

The **Main Map** presented in this paper, with the main geomorphological map at 1:7,500 scale, includes four main sections:

- (1) An orography section (on the upper part);
- (2) A geological map section (on the upper right part);
- (3) A main geomorphological map section (in the central left part);
- (4) A multi-temporal analysis section (in the lower part).

## 2. Study area

The study area is located in the piedmont-hilly area of the Abruzzo Region, stretching from the eastern slope of the chain (Maiella Massif) up to the Adriatic coast (about 20 km away). It is a typical hilly area with heights ranging from 150 to 450 m a.s.l., dissected by N-S-trending valleys (Dendalo and Vesola Rivers).

The Adriatic piedmont fringes the easternmost ridges of the chain, which is mainly represented by carbonate platform, slope, and pelagic basin sequences. It is characterized by a low-relief hilly landscape carved on sin- and late-orogenic deposits of the turbiditic foredeep sequences, largely covered and unconformably overlain by Pleistocene hemipelagic sequences. Post-orogenic deposits merely consist of slope, fluvial, and alluvial fan deposits (Figure 2). The marine environment persisted until the Early Pleistocene, when the regional north-eastward tilting of the area, subsequent to the main thrusting phase (Ascione, Cinque, Miccadei, Villani, & Berti, 2008), led to a sub-parallel (SW–NE) arrangement of the main valley across the emerged coastal plain (D’Alessandro, Miccadei, & Piacentini, 2003; Piacentini et al., 2018).

The present-day tectonic setting is dominated by extensional tectonics which is still active in the axial part of the chain as confirmed by several earthquakes (up to M 6.0; e.g. Majella Massif, 1933; Gran Sasso Massif, 1950; L’Aquila, 2009; Amatrice, 2016). The Apennines piedmont is characterized by moderate uplifting and seismicity (M 4–5; e.g. Orsogna, 1881; Torrecchia Teatina, 1992), while the Adriatic Sea is affected by subsidence and by moderate compression and strike-slip related seismicity (M 4–5; e.g. Abruzzo-Marche coast, 1987) (Rovida, Locati, Camassi, Lolli, & Gasperini, 2016) (Figure 2).

The geomorphological evolution of the Abruzzo piedmont sector is strongly controlled by the Late Miocene building of the Apennine thrust belt and by the recent evolution of the Apennine chain. The above-mentioned tectonic features, together with the eustatic fluctuations of the sea level, control the trend of the leading drainage lines and morphological



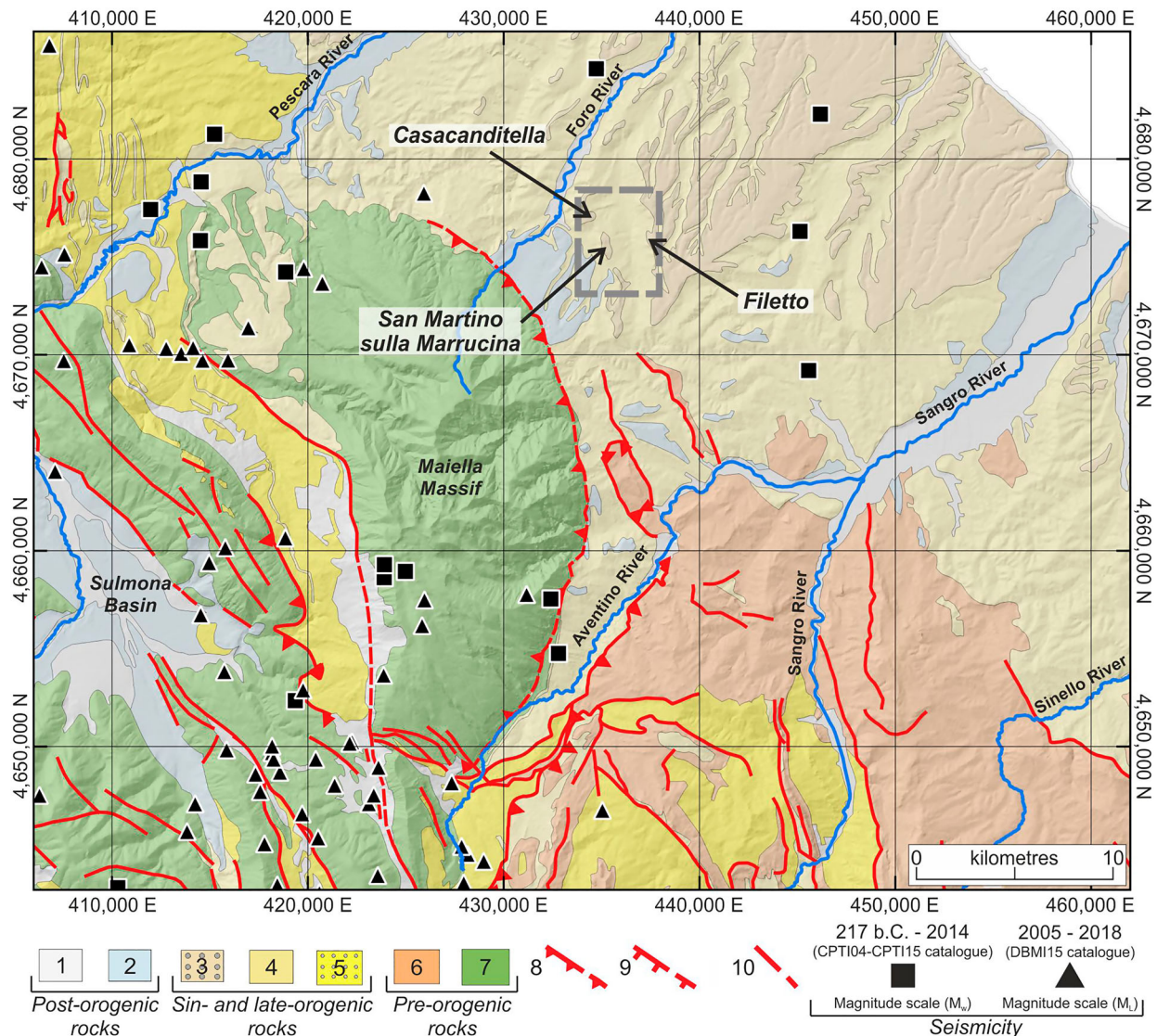


**Figure 2.** Geological sketch of central-eastern Abruzzo (modified from Carabella et al., 2019). Legend: post-orogenic rocks – (1) fluvial deposits (Holocene), (2) fluvial deposits (Middle-Late Pleistocene); sin- and late-orogenic rocks – (3) marine to continental transitional sequences (Early Pleistocene), (4) hemipelagic sequences with conglomerate levels (Late Pliocene–Early Pleistocene), (5) turbiditic foredeep sequences (Late Miocene–Early Pliocene); pre-orogenic rocks – (6) pelagic sequences (Oligocene–Miocene), (7) carbonate platform, slope and pelagic basin sequences (Jurassic–Miocene); (8) major thrust (dashed if buried); (9) major normal fault (dashed if buried); (10) major fault with strike-slip or reverse component (dashed if buried); seismicity – CPTI04 (Gruppo di Lavoro, 2004)–CPTI15 (Rovida et al., 2016) catalogue (black square); DBMI15 (Locati et al., 2016) catalogue (black triangle). The gray dashed box indicates the location of the study area.

ridges of the investigated area (D’Alessandro et al., 2003; Parlagraeco et al., 2011). In particular, the shaping of the reliefs and the geomorphological evolution of this sector of the region are directly connected to slope movements (Bozzano et al., 2017; Calista et al., 2019; Centamore, Nisio, Prestininzi, & Scarascia Mugnozza, 1997).

### 3. Methods

A detailed-scale geomorphological analysis, combined with the morphometric analysis of the area, allowed to realize large-scale maps of San Martino sulla Marrucina’s landslides.

Vectorial topographic data (1:5,000 and 1:10,000 scale) were retrieved from the Open Data service

(<http://opendata.regione.abruzzo.it/>) of Abruzzo Region (2007a, 2007b), and a 5 m cell Digital Terrain Model (DTM) was processed; furthermore, LiDAR data (1 m resolution) was provided for this study by Ministero dell’Ambiente e della Tutela del Territorio e del Mare (<http://www.minambiente.it/>). The morphometric analysis was carried out with the GIS software (QGIS 2018, version 3.4 ‘Madeira’), involving the analysis of the main orographic features, such as elevation analysis, slope analysis, aspect analysis (Strahler, 1952), and local relief analysis (sensu Ahnert, 1984, elevation range in a 500 m<sup>2</sup> window).

Geological and geomorphological analyses were based on field mapping, integrated with available literature data (i.e. Piano di Assetto Idrogeologico – PAI – database; Abruzzo-Sangro Basin Authority, 2005;

Inventario dei Fenomeni Franosi in Italia – IFFI – database; ISPRA, 2007a), stereoscopy, and air-photo interpretation. A detailed field mapping was carried out to investigate lithological features, superficial deposit cover, and the type of and distribution of geomorphological landforms, especially landslides. Information on lithology and thickness of bedrock and superficial deposits were also achieved through the analysis of boreholes.

The mapping was performed according to the guidelines of the Geological Survey of Italy and AIGeo (Italian Association of Physical Geography and Geomorphology) and thematic literature (Hungri, Leroueil, & Picarelli, 2014; ISPRA, 2007b; Varnes, 1978; WP/WLI, 1993, 1995); the geomorphological legend used in this work was conceived on the basis of the aforesaid guidelines, in order to better represent the features of the study area. Where available, the bedrock covered by deposits was reconstructed through boreholes data, by the use of a GIS-aided correlation and interpolation; this analysis allowed the generation of the depth-contour (0,5 m spacing), which represents the thickness of continental deposits and the isopach of the top surface of the Plio-Pleistocene marine deposits (zoomed map in the geological map section).

Air-photo interpretation was accomplished by using the 1:33,000 (Flight GAI 1954 – IGMI, 1954; Flight Abruzzo Region 1981–1987 – Abruzzo Region, 1987), and the 1:13,000 scale (Flight Abruzzo Region 2001–2002 – Abruzzo Region, 2002) stereoscopic air-photos and the 1:5,000 scale (Abruzzo Region, 2010) orthophoto color images. Combined with the field mapping, this results supported the geomorphological investigation of the study area. The primary goal was to properly define a landslide inventory for the study area, by characterizing each detected phenomenon in terms of landslide types (Hungri et al., 2014; Varnes, 1978) and providing a preliminary indication about the state of activity according to WP/WLI (1993). Landslides were mapped, according to their activity, into three main categories: active, dormant, and stabilized.

In order to further understand the evolution of the landslide area, a dendrochronological analysis was carried out, by sampling 12 trees. All samples were examined through the standard dendrochronological dating procedure using: preparation of samples on wooden supports, smoothing, first dating via skeleton plot, tree rings measuring with micrometric sled (precision 1  $\mu$ ), statistical control via Cofecha software (Holmes, 1983), ring growth curves and eccentricity analysis of the stem, up to the visual detection and classification of growth anomalies with Schweingruber, Eckstein, Serre-Bachet, and Bräker (1990) method.

To improve the knowledge of spatial and temporal evolution of landslides in the study area, an interferometric analysis was implemented. The approach used

in this work is the so-called Persistent Scatterers Interferometry (PSI), which is based on the information achieved by pixels of the SAR images characterized by high coherence over long time intervals (Ferretti et al., 2001; Hooper, Zebker, Segall, & Kampes, 2004; Kampes, 2006). Generally, constructed structures, such as buildings, bridges, dams, railways, pylons, or natural elements, such as outcropping rocks or homogeneous terrain areas, can represent good Persistent Scatterers (PS).

For the present case study, we performed A-DInSAR analyses of past displacements using four SAR data-stacks from the ESA archive ranging in the period 1992–2010. Specifically, ERS1/2 and Envisat data were selected respectively for 1992–2001 period and 2002–2010 period; using the ERS and Envisat A-DInSAR results, which provided quantitative data (i.e. the detection of targets affected by displacements), the landslide state of activity for the two analyzed temporal periods was assessed. Since landslides are located on both west- and east-facing slopes, even if PS data are available for both dataset results, displacements are sometimes visible in only one of them because of the direction of the Line of Sight (LOS). Therefore, the consideration of both geometries (ascending and descending) allows the detection of displacements that might go unseen by using only one geometric condition.

## 4. Results

The enclosed map shows the main features of the area and incorporates four sections, described in the following paragraphs.

### 4.1. Orography section

The study area reaches its maximum altitude in the westernmost and easternmost sectors, in correspondence of the tabular reliefs on which the principal villages rise (>400 m a.s.l.); this landscape is interrupted by the Dendalo River valley, where lower altitudes (up to 150 m a.s.l.) are reached. The study area shows a homogeneous slope distribution (about 5°–15°), with some peaks (>20°) especially in correspondence of the steep structural scarps, which border the tabular reliefs, and in correspondence of some secondary scarps along the slopes; along these areas, also the values of the local relief are maximum (~200 m).

### 4.2. Geological map section

On the geological map, outcropping lithologies were classified by their general sedimentary environments in bedrock lithologies and Quaternary continental deposits. They are listed in the following paragraphs, from the oldest to the youngest (ISPRA, 2010).



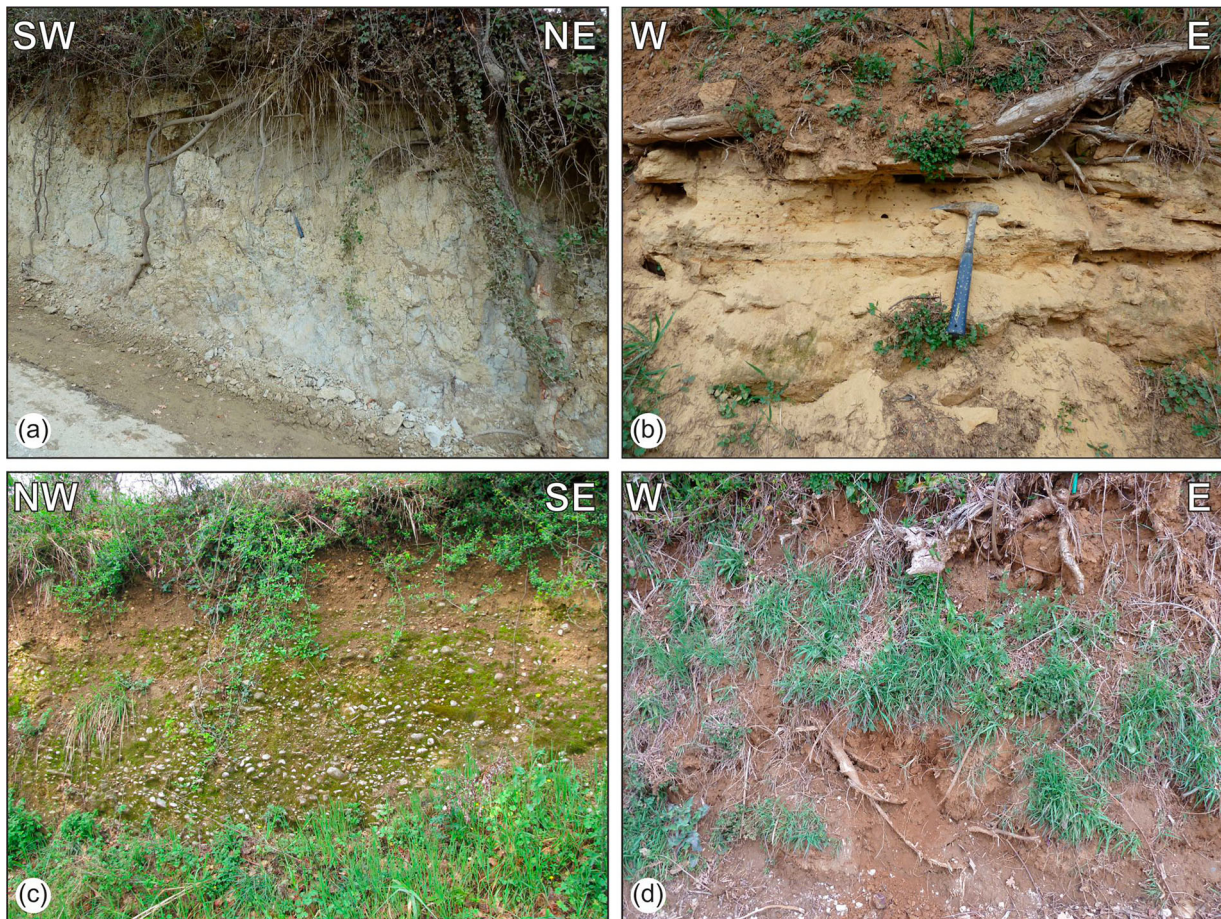


**Figure 3.** Lithologies of the study area: (a) mainly pelitic deposits of the Mutignano Formation, near Cipriani; (b) mainly sandy deposits of the Mutignano Formation, at C.le Madonna; (c) pelitic unit with intercalation of gravels, belonging to the Filetto clays and conglomerates, near C.le Saraceno; (d) Eluvial-colluvial covers, at C.le Madonna.

#### 4.2.1 Bedrock lithology (upper Pliocene – upper Pleistocene)

The bedrock includes two lithologies referable to marine deposits and one to marine to continental transitional deposits (Figure 3).

- Mutignano formation: (b) – Clays and silty clays from gray to azure-gray, in thin and very thin layers with planar-laminations. They are alternated with sands and silty sands from gray to yellow, in thin and very thin layers generally with planar- or low angle cross-laminations. (a) – Fine-grained sands and silty sands from gray to yellow, loose or poorly cemented, in thin and medium layers, often with planar- or low angle cross-laminations. Frequently intercalations of fine-grained sandstones from gray to yellow are present in thin and very thin layers, and polygenic conglomerates, in medium and thick layers. Total outcropping thickness is higher than 300 m. They are neritic platform deposits, progressively passing to shore sediments.
- Filetto clays and conglomerates: Silty clays and clayey silts from gray to green, massive or thinly bedding. Presence of polygenic gravels with massive or planar bedding, in gray or yellow sandy

matrix. Often, they pass to sands and silty sands from gray to yellow, mainly with cross-bedding. Thickness is generally of few meters, rarely exceeding 25 m. They are lagoon and coastal lake deposits, often interbedded by fluvial-delta sediments.

#### 4.2.2 Quaternary continental deposits

The deposits include a Pleistocene to Holocene fluvial deposits sequences, consisting of three levels, and two levels of near-surface Holocene deposits of various nature.

- Col di Lana conglomerates: Polygenic conglomerates with planar- and cross-bedding, with gray sandy or silty-sandy matrix. They outcrop on fluvial terraces placed between 80 and 100 m above the present valley floor. Outcropping thickness varies from 30 to 35 m.
- Santa Lucia conglomerates: Polygenic conglomerates with planar- and cross-bedding, with gray sandy or silty-sandy matrix, with occasional lenses of clays and peats. They outcrop on fluvial terraces placed between 10 and 25 m above the present valley floor. Outcropping thickness is variable from 15 to 30 m.

- Present and recent alluvial deposits: Sands and silty sands from gray to brown, massive or thinly bedding. There are many lenses or layers of polygenic gravels, generally massive, with gray sandy or silty-sandy matrix. Thickness is variable from 3 to 5 m.
- Eluvial-colluvial covers (Figure 3(d)): Sandy-clayey silts from brown to dark, generally massive, with common vegetal remains and local polygenic gravels of centimetric size. There are occasional levels of silty-clayey sands from brown to yellow, arenaceous fragments, and local polygenic gravels of centimetric size. Sometimes they are involved in the landslide. Thickness varies from 1 to ~8 m (see the eluvial-colluvial cover thickness map).
- Landslide deposits: Chaotic accumulation of different materials according to the landslide source deposits. It may include especially pelitic-arenaceous, clayey, and gravel deposits.

#### 4.2.3 Structural-tectonic elements

The study area is marked by extensional tectonics (high angle or sub-vertical normal and transpressive faults) that dismembered and displaced the Plio-Pleistocene formations. They generally have a limited length, and the corresponding upthrow ranges between few meters and few tens of meters.

According to the high erodibility of outcropping lithologies, and the strong thicknesses of the colluvial covers, it was not possible to detect any evidence of tectonic deformation. Therefore, the analysis and identification of the main fault alignments were done by using morphological analysis, photointerpretation, and stratigraphic data, which highlight local repetitions of the sedimentary series or dislocations of the main lithological contacts.

The main fault systems show a N-S, E-W, SW-NE, SE-NW, and SSE-NNW trend. The principal elements, relating to the N-S and SSE-NNW systems, are responsible for the configuration of the main drainage pattern and major ridges of the area, determining the progressive lowering of the Mutignano Formation towards the Dendalo River valley, as clearly evident near Casa dell'Arciprete. Secondary elements with E-W, SE-NW, and SW-NE direction are responsible for the displacement of the stratigraphic contact between sandy and pelitic portion of the Mutignano Formation, progressively lowered towards N. These elements are often found in the same direction of secondary watercourses and minor ridges (see structural scheme in the map).

#### 4.3. Geomorphological map section

The study area is characterized by several landforms, heterogeneously distributed according to the morphological, hydrographic, and lithological setting (Figure 4).

Regarding the structural landforms, besides the structural alignments described in the previous paragraph, structural surfaces are present. They are the top of the tabular relief, where mainly sandy and ruditic deposits outcrop, and surrounded by steep structural slopes.

Landslides are the main landforms of the study area. Most of the phenomena can be highlighted in the central sector of the map, along the slope of the Dendalo River valley, while they are rare outside this basin. Field surveys and photointerpretation analysis showed that the slope landforms are hardly distributed as isolated phenomena, but they occur mainly as complex landslide systems, where it is often difficult to distinguish and to map each event.

Slides and complex landslides mainly show a roto-translational sliding surface, as highlighted by counterslopes and counterscarps recognized in landslide bodies; however, the geometry of the sliding surfaces shows a strong structural control, mainly connected to fault zones and bedding planes. In fact, analyzing the structural scheme, it can be noticed that most of the main landslide scarps and flanks coincide with faults or with morphological alignments deduced from photogeology (see structural scheme in the map). Furthermore, near the main structural features, the scarps show a sub-rectilinear trend, while far from these elements, they show a concave shape. Landslide scarps have different morphological and geomorphological characteristics: where the pelitic deposits outcrop, they are highly degraded, while where sandy deposits are present, they are fresh and evident. The geometry of the sliding surfaces, especially in the middle and lower part of the deposit, is conditioned by the bedding of the pelitic sequences, and they follow the anisotropies present in the landslide body, up to the valley floor.

Most landslides are in active state, even if dormant or stabilized landslides are present. In particular, dormant landslides generally have small sizes, while stabilized landslides have greater dimensions and are present in the northeastern areas, along the northwestern slope of Filetto, near C.le Saraceno. The most extensive landslides are represented by earth slides and complex landslides characterized by deep failure surfaces, often in the range of several tens of meters. The smaller instability phenomena, represented by earth flows, are rare and generally involve only the continental deposits, with failure surfaces few meters deep. Landslides mostly show very low deformation rates.

Finally, local processes related to viscous deformation of shallow material (creep and/or solifluction) affect the steeper slopes or portions of slopes surrounding the landslide areas, where the eluvial-colluvial cover is thicker, and the action of running waters is greater, especially in correspondence of down-cutting streams and gullies. These active processes show very low



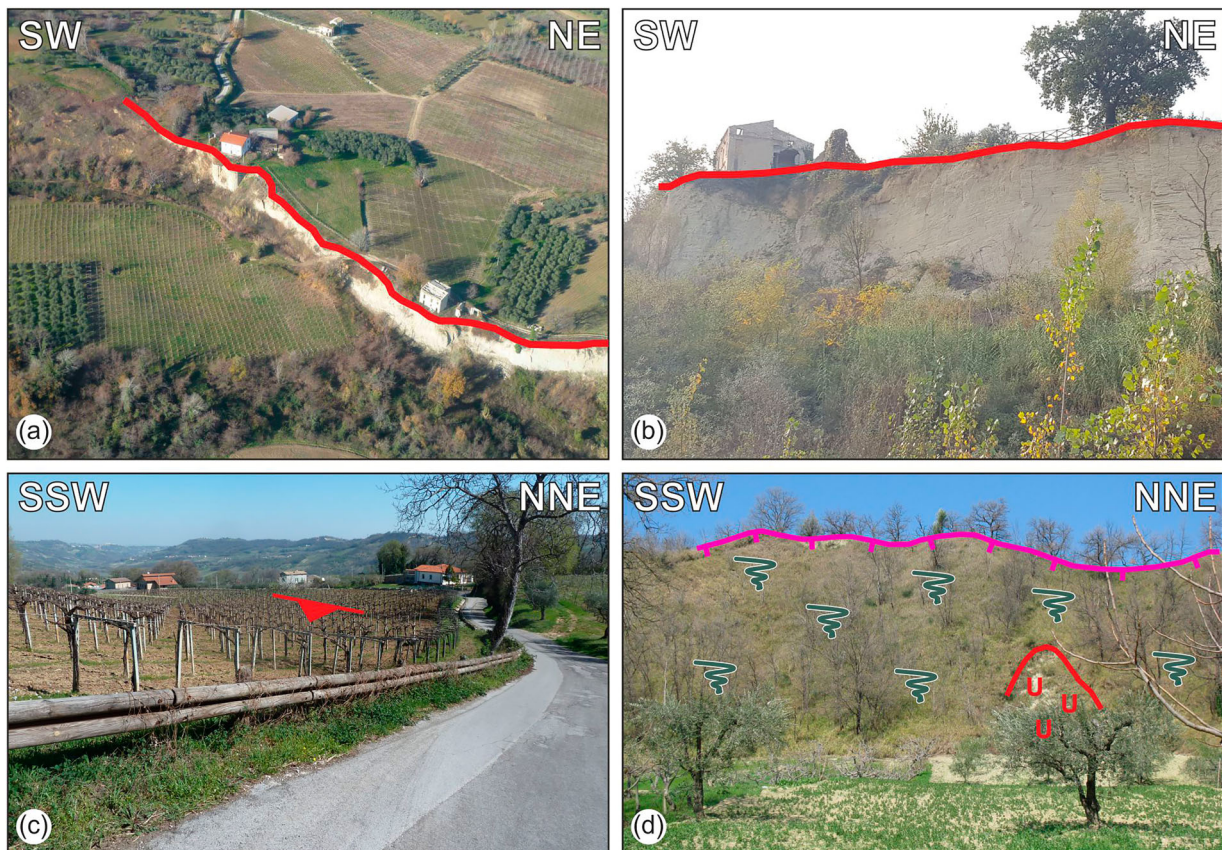


**Figure 4.** Geomorphological features of the study area; (a) aerial view of a landslide scarp, near Casa dell'Arciprete; (b) detail of the northeastern part of the previous scarp (a), with outcrops of pelitic deposits; (c) landscape view of the counterslope inside the active earth slide near Piano Palomba; (d) Polygenic scarp with clear structural origin but currently affected by landslide phenomena and diffuse runoff and erosion, on the eastern slope of Casacanditella.

deformation rates and involve only the superficial deposits for thicknesses of about 1 or 2 m.

The fluvial landforms are characterized by the main watercourses and its tributary, marked by deepening tendency (down-cutting stream, gully erosion, and widespread runoff area), and by some depositional landforms, as the alluvial fan (especially in the external part of the map). The high erodibility of the lithologies of the study area leads to the accumulation of abundant eluvial-colluvial covers, along with the most extensive reliefs.

#### 4.4 Geomorphological cross-sections

Geomorphological and available stratigraphic information on key areas were synthesized in three cross-sections (lower portion of the map), chosen in order to best demonstrate the geometry of the bedrock and landslide bodies.

The profiles clearly display how the landslides are in close connection with each other, often presenting several coalescent bodies. Furthermore, they outline the strong thicknesses (up to 60–70 m) of the most extensive landslides, while the smaller landslides generally interest only the Quaternary continental deposits.

The geomorphological sections highlight the overall slope deformation behavior: the northern sections

(1–1' and 2–2') are primarily characterized by horizontal displacements, especially near to the landslide foot, as typical for this type of earth compound slide. Instead, the southern section (3–3') results affected by slightly stronger vertical displacements, especially very near to the scarps of the lowest landslide body.

#### 4.5 Dendrochronological analysis

All the sampling data and growth anomalies found, involving a time interval at most 92 years (1920–2012), are summarized in Table 1.

Oaks in the northern area (3–4), showed no anomaly related to recent reactivations, while those located in the central part (7–8–9), clearly showed more than one growth stress, linked to the movement reactivation in 1968, 1981 and 2002. Some of these trees have been strongly disturbed, producing very small rings for a few decades, and sometimes more than once (i.e. tree 8; Figure 5). Control trees (11–12) didn't show any growth anomalies.

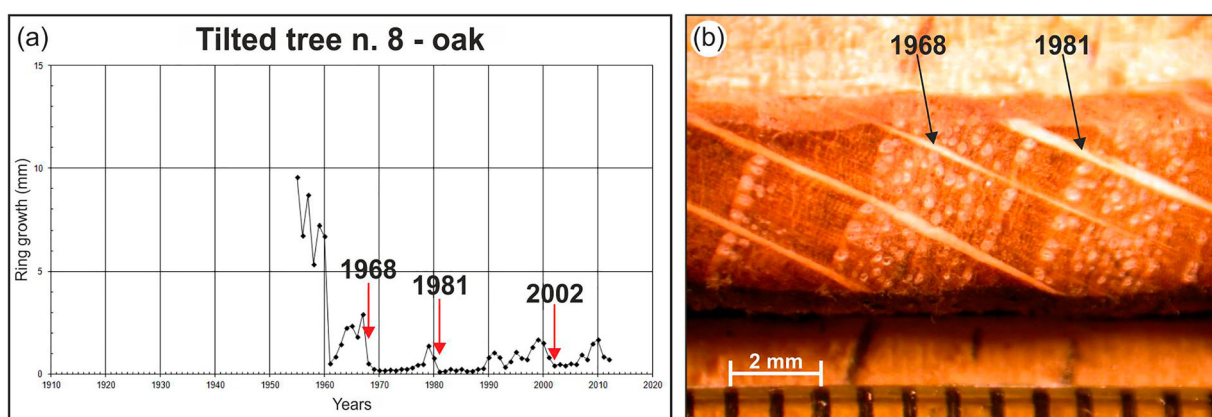
#### 4.6 Interferometric analysis

In order to achieve more quantitative information about the recent geomorphological evolution of the landslide area, an analysis by multi-temporal Advanced



**Table 1.** Dendrochronological analysis for the twelve sampled trees (for samples' location see borehole and dendrochronology section).

Tree n.	Sample n.	Orientation inclination trunk (°)	Trunk inclination from vertical (°)	Direction of sampling	Species	Range examined	Period with anomalies	Reduction growth intensity	Notes
1	1	N 195	25	N195	walnut	1993–2012	2007–2012	51–70%	Sprout dating
1	1b	Vertical		N010	walnut	2006–2012			
2	2	N 242	20	N240	walnut	1986–2012			
3	3	Vertical		N060	oak	1962–2012			
4	4	Vertical		N280	walnut	1986–2012			
5	5	Vertical		N255	oak	1939–2012			
6	6	N 240	30	N240	walnut	1959–2012	1976		Eccentricity
7	7	Vertical		N250	oak	1930–2012	1968–1977	51–70%	3 stress time intervals
8	8	N 90	40	N250	oak	1955–2012	1698–1978	>70%	
						1981–1989	>70%		
9	9	N120	32	N120	oak	1944–2012	1968–1975	51–70%	2 stress time intervals
							1980–1988	51–70%	
10	10	N110	10	N110	oak	1981–2012			
11	11	Vertical		N040	oak	1920–2012			Control
12	12	Vertical		N290	oak	1965–2012			Control

**Figure 5.** Dendrochronological analysis for tree sample n. 8: (a) ring growth curve; (b) growth stress.

Differential SAR Interferometry (A-DInSAR) was performed on four datasets of archive satellite C-band SAR images acquired by the European Space Agency (ESA) from 1992 up to 2010 (see interferometry section). More in detail ERS1/2 data have been selected for the period 1992–2001, and Envisat data for the period 2002–2010. Both ERS and Envisat data-stacks, in double orbital geometry (Ascending and Descending), have been processed by using Persistent Scatterers-like (PS) methodologies.

PSs colors on the map are related to displacement rates (mm/year) along the Line of Sight (LOS): dots from yellow to red show displacements away from the satellite, and dots from light blue to dark blue indicate displacements towards the satellite; green dots represent points not showing displacement observed by the satellite during the investigated period.

PSs do not show significant displacements over the urban areas, and so we derived that almost all landslide processes seemed not to affect such villages. Nearer to the valley floor, the slopes degrade gently, and especially on the western slopes, many PSs show displacement information in both the ascending and descending geometries (especially near Piano Palomba).

For both the ERS and Envisat periods, green polygons define landslides characterized by the presence of stable PSs (negligible velocity), whereas red polygons identify the presence of unstable PSs. Empty polygons indicate landslides with missing or insufficient PSs. Through the analysis of stable and unstable PSs, the state of activity of every mapped process was supposed, as shown in the state of activity matrix (Table 2).

## 5. Conclusion

The San Martino sulla Marrucina landslides were investigated through a combination of detailed geological and geomorphological field surveys, air-photo interpretation, GIS analysis of DTMs (hillshade, slope, aspect, local relief thematic layers), boreholes

**Table 2.** State of activity matrix, modified from Bozzano et al. (2017) (colors refer to the legend in the interferometry section).

		ASCENDING GEOMETRY		
		Unstable PS	Stable PS	Not enough PS
DESCENDING GEOMETRY	Unstable PS	Active	Active	Active
	Stable PS	Active	Stabilized	Undefined
	Not enough PS	Active	Undefined	Undefined

data, dendrochronological and interferometric analyses. The combination of these data proved to be fundamental for the accuracy of the Main Geomorphological Map.

The acquired data suggest a complex nature for the San Martino sulla Marrucina landslides, which are characterized by a very rough topography (e.g. scarps, ridges, counterslope, down-cutting streams, ponds, etc.), documenting the activity of long-term landslide processes. This conclusion was inferred by:

- the photogeological analysis, which allowed the definition of the spatial and temporal evolution of the instability processes over the last five decades (1954–2010);
- the detailed geomorphological analysis (updated to 2019), which showed that the landslides are often composed of several coalescent bodies;
- the dendrochronological analysis, which highlighted several gravitational movements in a time window of about 90 years (1920–2012);
- the satellite A-DInSAR analysis, which enabled the observation of the deformation affecting both the East and West facing slopes in an 18-year period (1992–2010), with rather low speeds, but locally even higher than 20 mm/year.

Furthermore, the multi-temporal displacement data, deduced from the dendrochronological and interferometric analyses, allowed us to infer the state of activity of the landslides. These data confirmed, together with the geomorphological field survey, the active status for most of the landslides, especially in the left valley side; most of these landslides are characterized by very slow movement, which can be detected through dendrochronological and interferometric analyses. Only the more southern landslides, in the southeastern slope of San Martino sulla Marrucina, show clear indications of reactivation over the last few years, as also confirmed in the analyses carried out on aerial photographs after 2002. The landslides in dormant status show periodic cycles of reactivation that vary from a few years to a few decades.

### Software

The vector/raster data and main map were managed using QGIS 3.4 Madeira<sup>®</sup>, with final editing performed using Corel Draw 2019<sup>®</sup>.

### Acknowledgment

The authors wish to thank the Struttura Speciale di Supporto Sistema Informativo Regionale (<http://www.regione.abruzzo.it/xcartografia/>) and the Open Geodata service (<http://opendata.regione.abruzzo.it/>) of Abruzzo Region for providing the topographic data and aerial photos used for the geomorphological investigations. The 20 m SINAnet (Sistema

Informativo Nazionale Ambientale) DEM was provided by ISPRA (<http://www.sinanet.isprambiente.it/it/sia-ispra/download-mais/dem20/view>), LIDAR is provided by Ministero dell'Ambiente e della Tutela del Territorio e del Mare (<http://www.minambiente.it/>), and Urban areas are provided by ISTAT (<https://www.istat.it/it/archivio/104317>). The authors are also grateful to the reviewer W. Frodella, A. Chelli, and A. Labetski, whose suggestions greatly improved the manuscript and map.

### Disclosure statement

No potential conflict of interest was reported by the authors.

### Funding

The work was supported by Università degli Studi 'G. d'Annunzio' Chieti Pescara funds (E. Miccadei University funds).

### ORCID

Francesca Bozzano  <http://orcid.org/0000-0002-0297-842X>

Cristiano Carabella  <http://orcid.org/0000-0001-9206-2812>

Marco Emanuele Discenza  <http://orcid.org/0000-0001-8534-9989>

Paolo Mazzanti  <http://orcid.org/0000-0003-0042-3444>

Enrico Miccadei  <http://orcid.org/0000-0003-2114-2940>

Alfredo Rocca  <http://orcid.org/0000-0002-7750-4237>

Nicola Sciarra  <http://orcid.org/0000-0002-0554-415X>

### References

- Abruzzo Region. (1987). 1:33,000 scale aerial photos of Flight Abruzzo Region 1981–1987. Retrieved from [http://geoportale.regione.abruzzo.it/Cartanet/pages4home/foto\\_aeree/volo-regione-abruzzo-1982-84-1985-87](http://geoportale.regione.abruzzo.it/Cartanet/pages4home/foto_aeree/volo-regione-abruzzo-1982-84-1985-87)
- Abruzzo Region. (2002). 1:13,000 scale aerial photos of Flight Abruzzo Region 2001–2002. Retrieved from [http://geoportale.regione.abruzzo.it/Cartanet/pages4home/foto\\_aeree/volo-regione-abruzzo-2001-2002](http://geoportale.regione.abruzzo.it/Cartanet/pages4home/foto_aeree/volo-regione-abruzzo-2001-2002)
- Abruzzo Region. (2007a). 1:5,000 scale regional technical maps. L'Aquila: Struttura Speciale di Supporto Sistema Informativo Regione Abruzzo. Retrieved from <http://opendata.regione.abruzzo.it/content/dbtr-regione-abruzzo-scala-15000-edizione-2007-formato-shp>
- Abruzzo Region. (2007b). 1:10,000 scale regional topographic maps. L'Aquila: Struttura Speciale di Supporto Sistema Informativo Regione Abruzzo. Retrieved from <http://opendata.regione.abruzzo.it/content/dbtr-regione-abruzzo-scala-110000-edizione-2007-formato-shp>
- Abruzzo Region. (2010). 1:5,000 scale orthophotos color images. L'Aquila: Struttura Speciale di Supporto Sistema Informativo Regione Abruzzo. Retrieved from <http://opendata.regione.abruzzo.it/content/ortofoto-digitale-della-provincia-di-laquila>
- Abruzzo-Sangro Basin Authority. (2005). Piano Stralcio di Bacino per l'Assetto Idrogeologico dei Bacini di Rilievo Regionale Abruzzesi e del Bacino del Fiume Sangro. (L.R. 18.05 1989 n.81 e L. 24.08.2001) – Carta geomorfologica – scala 1:25.000. Retrieved from <http://autoritabacini.regione.abruzzo.it/index.php/carta-geomorfologica-pai>



- Ahnert, F. (1984). Local relief and the height limits of mountain ranges. *American Journal of Science*, 284(9), 1035–1055. doi:10.2475/ajs.284.9.1035
- Akbarimehr, M., Motagh, M., & Haghshenas-Haghighi, M. (2013). Slope stability assessment of the sarcheshmeh landslide, northeast Iran, investigated using InSAR and GPS observations. *Remote Sensing*, 5(8), 3681–3700. doi:10.3390/rs5083681
- Aleotti, P., & Chowdhury, R. (1999). Landslide hazard assessment: Summary review and new perspectives. *Bulletin of Engineering Geology and the Environment*, 58, 21–44. doi:10.1007/s100640050066
- Amato, V., Aucelli, P. P. C., Bellucci Sessa, E., Cesarano, M., Incontri, P., Pappone, G., ... Vilardo, G. (2017). Multidisciplinary approach for fault detection: Integration of PS-InSAR, geomorphological, stratigraphic and structural data in the Venafro intermontane basin (Central-Southern Apennines, Italy). *Geomorphology*, 283, 80–101. doi:10.1016/j.geomorph.2017.01.027
- Ascione, A., Cinque, A., Miccadei, E., Villani, F., & Berti, C. (2008). The Plio-Quaternary uplift of the Apennine chain: New data from the analysis of topography and river valleys in Central Italy. *Geomorphology*, 102(1), 105–118. doi:10.1016/j.geomorph.2007.07.022
- Bardi, F., Frodella, W., Ciampalini, A., Bianchini, S., Del Ventisette, C., Gigli, G., ... Casagli, N. (2014). Integration between ground based and satellite SAR data in landslide mapping: The San Fratello case study. *Geomorphology*, 223, 45–60. doi:10.1016/j.geomorph.2014.06.025
- Bozzano, F., Mazzanti, P., Perissin, D., Rocca, A., De Pari, P., & Discenza, M. E. (2017). Basin scale assessment of landslides geomorphological setting by advanced InSAR analysis. *Remote Sensing*, 9(3), 267. doi:10.3390/rs9030267
- Brunetti, M. T., Peruccacci, S., Rossi, M., Luciani, S., Valigi, D., & Guzzetti, F. (2010). Rainfall thresholds for the possible occurrence of landslides in Italy. *Natural Hazards and Earth System Science*, 10(3), 447–458. doi:10.5194/nhess-10-447-2010
- Calista, M., Miccadei, E., Piacentini, T., & Sciarra, N. (2019). Morphostructural, meteorological and seismic factors controlling landslides in weak rocks: The case studies of Castelnuovo and Ponzano (North East Abruzzo, Central Italy). *Geosciences*, 9(3), 122. doi:10.3390/geosciences9030122
- Carabella, C., Miccadei, E., Paglia, G., & Sciarra, N. (2019). Post-wildfire landslide hazard assessment: The case of the 2017 Montagna Del Morrone Fire (Central Apennines, Italy). *Geosciences*, 9(4), 175. doi:10.3390/geosciences9040175
- Centamore, E., Nisio, S., Prestinanzi, A., & Scarascia Mugnozza, G. (1997). Evoluzione morfodinamica e fenomeni franosi nel settore periadriatico dell'Abruzzo settentrionale. *Studi Geol Camerti*, 14, 9–27.
- Ciulli, M., Bezzi, M., Comunello, G., Laitempergher, G., Gobbi, S., Tattoni, C., & Cantiani, M. G. (2019). Integrating dendrochronology and geomatics to monitor natural hazards and landscape changes. *Applied Geomatics*, 11(1), 39–52. doi:10.1007/s12518-018-0236-0
- Coulthard, B. L., & Smith, D. J. (2013). Dendrochronology. In *Encyclopedia of quaternary science: Second edition*. doi:10.1016/B978-0-444-53643-3.00355-1
- Dai, F. C., Lee, C. F., & Ngai, Y. Y. (2002). Landslide risk assessment and management: An overview. *Engineering Geology*, 64(1), 65–87. doi:10.1016/S0013-7952(01)00093-X
- D'Alessandro, L., Miccadei, E., & Piacentini, T. (2003). Morphostructural elements of central-eastern Abruzzi: Contributions to the study of the role of tectonics on the morphogenesis of the Apennine chain. *Quaternary International*, 101–102, 115–124. doi:10.1016/S1040-6182(02)00094-0
- Del Ventisette, C., Righini, G., Moretti, S., & Casagli, N. (2014). Multitemporal landslides inventory map updating using spaceborne SAR analysis. *International Journal of Applied Earth Observation and Geoinformation*, 30(1), 238–246. doi:10.1016/j.jag.2014.02.008
- Fantucci, R., & Sorriso-Valvo, M. (1999). Dendrogeomorphological analysis of a slope near Lago, Calabria (Italy). *Geomorphology*, 30, 165–174. doi:10.1016/S0169-555X(99)00052-5
- Ferretti, A., Prati, C., & Rocca, F. (2001). Permanent scatterers in SAR interferometry. *IEEE Transactions on Geoscience and Remote Sensing*, 39(1), 8–20. doi:10.1109/36.898661
- Francioni, M., Calamita, F., Coggan, J., De Nardis, A., Eyre, M., Miccadei, E., ... Sciarra, N. (2019). A multi-disciplinary approach to the study of large rock avalanches combining remote sensing, GIS and field surveys: The case of the Scanno landslide, Italy. *Remote Sensing*, 11(13), 1570. doi:10.3390/rs11131570
- Gaidzik, K., Ramírez-Herrera, M. T., Bunn, M., Leshchinsky, B. A., Olsen, M., & Regmi, N. R. (2017). Landslide manual and automated inventories, and susceptibility mapping using LIDAR in the forested mountains of Guerrero, Mexico. *Geomatics, Natural Hazards and Risk*, 8(2), 1054–1079. doi:10.1080/19475705.2017.1292560
- Glade, T., Anderson, M., & Crozier, M. J. (2012). *Landslide hazard and risk*. Wiley, J. & Sons. doi:10.1002/9780470012659
- Gruppo di Lavoro. (2004). *Gruppo di Lavoro CPTI Catalogo Parametrico dei Terremoti Italiani, 2004 (CPTI04)*. Bologna, Italy: Istituto Nazionale di Geofisica e Vulcanologia (INGV).
- Höfle, B., & Rutzinger, M. (2011). Topographic airborne LiDAR in geomorphology: A technological perspective. *Zeitschrift Fur Geomorphologie*, 55, 1–29. doi:10.1127/0372-8854/2011/0055S2-0043
- Holmes, R. L. (1983). Computer-assisted quality control in tree-ring dating and measurements. *Tree-Ring Bulletin*, 43, 69–78.
- Hooper, A., Zebker, H., Segall, P., & Kampes, B. (2004). A new method for measuring deformation on volcanoes and other natural terrains using InSAR persistent scatterers. *Geophysical Research Letters*, 31, L23611. doi:10.1029/2004GL021737
- Hungr, O., Leroueil, S., & Picarelli, L. (2014). The Varnes classification of landslide types, an update. *Landslides*, 11(2), 167–194. doi:10.1007/s10346-013-0436-y
- IGMI. (1954). *1:33,000 scale aerial photos of Flight GAI*. Istituto Geografico Militare Italiano. Retrieved from [http://geoportale.regione.abruzzo.it/Cartanet/pages4home/foto\\_aeree/volo-base-i.g.m.-1954-56](http://geoportale.regione.abruzzo.it/Cartanet/pages4home/foto_aeree/volo-base-i.g.m.-1954-56)
- ISPRA. (2007a). Progetto IFFI-Inventario dei Fenomeni Franosi in Italia. Retrieved from [http://www.apat.gov.it/site/it-IT/Progetti/IFFI\\_-Inventario\\_dei\\_fenomeni\\_franosi\\_in\\_Italia/](http://www.apat.gov.it/site/it-IT/Progetti/IFFI_-Inventario_dei_fenomeni_franosi_in_Italia/)
- ISPRA. (2007b). Guida alla rappresentazione cartografica della Carta Geomorfologica d'Italia in scala 1:50,000. *Quaderni Serie III Del Servizio Geologico Nazionale*.
- ISPRA. (2010). Carta Geologica d'Italia alla scala 1:50,000, Foglio 361 'Chieti'. Servizio Geologico d'Italia. Retrieved from [http://www.isprambiente.gov.it/Media/carg/361\\_CHIETI/Foglio.html](http://www.isprambiente.gov.it/Media/carg/361_CHIETI/Foglio.html)

- Jaboyedoff, M., Oppikofer, T., Abellán, A., Derron, M. H., Loye, A., Metzger, R., & Pedrazzini, A. (2012). Use of LIDAR in landslide investigations: A review. *Natural Hazards*, 61(1), 5–28. doi:10.1007/s11069-010-9634-2
- Kampes, B. M. (2006). *Radar interferometry: Persistent scatterer technique*. Dordrecht, Netherlands: Springer, 213 p. doi:10.1007/978-1-4020-4723-7
- Locati, M., Camassi, R., Rovida, A., Ercolani, E., Bernardini, F., Castelli, V., ... Rocchetti, E. (2016). *DBMI15, the 2015 version of the Italian macroseismic database*. Rome, Italy: Istituto Nazionale di Geofisica e Vulcanologia (INGV).
- Parlagreco, L., Mascioli, F., Miccadei, E., Antonioli, F., Gianolla, D., Devoti, S., ... Silenzi, S. (2011). New data on Holocene relative sea level along the Abruzzo coast (central Adriatic, Italy). *Quaternary International*, 232, 179–186. doi:10.1016/j.quaint.2010.07.021
- Perissin, D., & Wang, T. (2012). Repeat-pass SAR interferometry with partially coherent targets. *IEEE Transactions on Geoscience and Remote Sensing*, 50(1), 271–280. doi:10.1109/TGRS.2011.2160644
- Peruccacci, S., Brunetti, M. T., Gariano, S. L., Melillo, M., Rossi, M., & Guzzetti, F. (2017). Rainfall thresholds for possible landslide occurrence in Italy. *Geomorphology*, 290, 39–57. doi:10.1016/j.geomorph.2017.03.031
- Peruccacci, S., Brunetti, M. T., Luciani, S., Vennari, C., & Guzzetti, F. (2012). Lithological and seasonal control on rainfall thresholds for the possible initiation of landslides in central Italy. *Geomorphology*, 139–140, 79–90. doi:10.1016/j.geomorph.2011.10.005
- Pezzo, M. I., & Dorigatti, S. (1999). Studi dendrocronologici in Italia: Un aggiornamento. *Ann Mus Civ*, 13, 143–161.
- Piacentini, T., Galli, A., Marsala, V., & Miccadei, E. (2018). Analysis of soil erosion induced by heavy rainfall: A case study from the NE Abruzzo hills area in Central Italy. *Water (Switzerland)*, 10(10), 1314. doi:10.3390/w10101314
- Rovida, A., Locati, M., Camassi, R., Lolli, B., & Gasperini, P. (2016). *CPTI15—2015 version of the parametric catalogue of Italian earthquakes*. Rome, Italy: Istituto Nazionale di Geofisica e Vulcanologia (INGV).
- Salvati, P., Bianchi, C., Rossi, M., & Guzzetti, F. (2010). Societal landslide and flood risk in Italy. *Natural Hazards and Earth System Science*, 10(3), 465–483. doi:10.5194/nhess-10-465-2010
- Schweingruber, F. H., Eckstein, D., Serre-Bachet, F., & Bräker, O. U. (1990). Identification, presentation and interpretation of event years and pointer years in dendrochronology. *Dendrochronologia*, 8, 9–38.
- Stefanini, M. C. (2004). Spatio-temporal analysis of a complex landslide in the Northern Apennines (Italy) by means of dendrochronology. *Geomorphology*, 63(3–4), 191–202. doi:10.1016/j.geomorph.2004.04.003
- Strahler, A. N. (1952). Dynamic basis of geomorphology. *Bulletin of the Geological Society of America*, 63, 923–938. doi:10.1130/0016-7606(1952)63[923:DBOG]2.0.CO;2
- Tofani, V., Raspini, F., Catani, F., & Casagli, N. (2013). Persistent Scatterer Interferometry (PSI) technique for landslide characterization and monitoring. *Remote Sensing*, 5, 1045–1065.
- Varnes, D. J. (1978). Slope movement types and processes. In R. L. Schuster & R. J. Krizek (Eds.), *Landslides, analysis and control*. Special Report; (pp. 11–33). Washington, DC: Transportation and Road Research Board, National Academy of Sciences.
- WP/WLI. (1993). A suggested method for describing the activity of a landslide. *Bulletin of the International Association of Engineering Geology*, 47, 53–57. doi:10.1007/BF02639593
- WP/WLI. (1995). A suggested method for describing the rate of movement of a landslide. *Bulletin of the International Association of Engineering Geology*, 52, 75–78. doi:10.1007/BF02602683